

# Relationship Between the Thermal Degradation Chemistry and Flammability of Commercial Flexible Polyurethane Foams

C. Denecker,<sup>1</sup> J. J. Liggat,<sup>1</sup> C. E. Snape<sup>2</sup>

<sup>1</sup>Department of Pure and Applied Chemistry, University of Strathclyde, 295 Cathedral Street, Glasgow G1 1XL, United Kingdom

<sup>2</sup>School of Chemical, Mining and Environmental Engineering, University of Nottingham, University Park, Nottingham NG7 2RD, United Kingdom

Received 25 October 2004; accepted 19 October 2005

DOI 10.1002/app.23701

Published online in Wiley InterScience (www.interscience.wiley.com).

**ABSTRACT:** In this article, we report the use of a variety of analytical methods, in particular, solid-state <sup>1</sup>H-NMR and <sup>13</sup>C-NMR to characterize the relationship between the condensed-phase chemistry and burning behavior as determined by a series of combustion tests for two commercially derived flexible polyurethane foams, one combustion-modified. The combustion tests showed that the foams met several regulatory requirements in terms of their fire performance, whether or not they were combustion-modified. Both foams passed the MV SS 302 and CAL 117 small-flame tests. The nonmodified foam failed the Crib 5 test, but this test had a much larger ignition source. The particular problem with the nonmodified foam was melt drip into the flame zone. This led to a steady maintenance of the fuel feed and a rapid escalation of the fire. In

contrast, the combustion-modified foam showed little melt drip and self-extinguished. Thermal analysis data for the two foams showed that melamine acted in part as an endothermic heat sink. This alone did not account for the much reduced melt flow and drip of the combustion-modified foam, but the solid-state <sup>1</sup>H-NMR data clearly showed that the molecular mobility of the combustion char from combustion-modified foam was lower than the unmodified foam char, which indicated that the flame-retardant formulation in the combustion-modified foam acted by a condensed-phase mechanism. © 2006 Wiley Periodicals, Inc. *J Appl Polym Sci* 100: 3024–3033, 2006

**Key words:** flame retardance; foams; NMR; polyurethanes; thermal properties

## INTRODUCTION

Synthetic polymer materials are part of modern life, and their ubiquity means that our fire safety depends, in part, on the fire behavior of these materials. Polyurethane (PU) foams are found in our homes, offices, and cars, and consequently, there have been a number of studies over the years on the thermal degradation behavior and flammability of urethane and related polymers.<sup>1</sup> Although the formulation of urethane-derived polymers is complex, the key features of their degradation chemistry have been identified. The degradation mechanisms of simple PUs derived from poly(ethylene glycol) and 4,4'-diisocyanato diphenylmethane (MDI) were studied in detail by Grassie and coworkers.<sup>2,3</sup> Under inert conditions, at temperatures above about 210°C, the PU linkage disappears without any volatile products being formed, and the initial degradation step is seemingly a simple depolymerization reaction. The two monomers

are the primary products, and all the other products, which include carbon dioxide, butadiene, tetrahydrofuran, dihydrofuran, and water as volatile products and carbodiimide and urea amide in the condensed phase, are formed from the monomers in a complex cascade of secondary reactions while they are diffusing from the hot polymer. This scheme has subsequently been confirmed by Ravey and Pearce,<sup>4</sup> Herzog,<sup>5</sup> and Jeffs and Sand.<sup>6</sup> Under oxidative conditions, Gaboriaud et al.<sup>7</sup> found that the first step involves the scission of the PU molecule into a primary amine, carbon dioxide, and propenyl ether species, with the latter leading to propene formation. The mechanism is reduced to a depolymerization process followed by the radical breakdown of the polyol chain in conjunction with simple radical formation. The radicals formed can explain the formation of the complex series of observed volatile products.

Melamine is widely used in the formulation of fire-retardant additive systems for flexible PU foams.<sup>8,9</sup> Its mode of action as a fire retardant is not well known, but it is believed to act as a heat sink with endothermic sublimation, providing noncombustible nitrogen-containing vapors.<sup>10–13</sup> These vapors probably dilute the fuel and are possibly chemically involved in the extinguishing process. In addition to simple sublima-

Correspondence to: J. J. Liggat (j.j.liggat@strath.ac.uk).

Contract grant sponsor: Huntsman Polyurethanes (Everberg, Belgium).

tion, melamine is known to undergo progressive endothermic condensation on heating with the elimination of ammonia (a flame diluent) and the formation of polymeric products called melam, melem, and melon.<sup>14–16</sup> When melamine is heated in an open system, it mostly sublimates unaltered above 250°C and leaves a small amount of residue (ca. 7%) of condensation products that are more thermally stable than melamine itself (melam to about 350°C, melem to about 450°C, and melon to about 600°C). However, in our recent investigation<sup>17</sup> with solid-state NMR techniques, we demonstrated that melamine has a pronounced condensed-phase effect in terms of the promotion of the formation of rigid char.

Tris(1-chloro-2-propyl)-phosphate (TCPP) is another common flame retardant for PU foams. Added in much lower quantities than melamine, it is often used in combination with melamine. It is believed to have both a gas-phase action (through the liberation of HCl) and a condensed-phase action (through the generation of phosphoric acid and derivatives).<sup>18</sup>

In the past, many mechanistic studies of polymer thermal degradation have been solely concerned with volatile products, with the condensed phase, often highly crosslinked even in the early stages of degradation, simply regarded as intractable. This principally reflects the limited availability of a suitable means of analyzing the residue. However, the advent of increasingly sophisticated solid-state NMR techniques, many of which were originally applied to structural studies of coal, has provided researchers with the opportunity for the direct and detailed characterization of condensed-phase chemistry.<sup>19–29</sup> Although solid-state <sup>13</sup>C-NMR is well-established as a technique for the structural elucidation of polymers, broad-line <sup>1</sup>H-NMR, which has a long history in the investigation of the mobility of coals and pitches during their carbonization,<sup>19–24</sup> is much less frequently encountered in polymer science. Indeed, its use in polymer thermal degradation studies has only relatively recently been reported.<sup>17</sup> For the broad-line <sup>1</sup>H-NMR of polymers, there are usually two contributions to the free-induction decay, one from a mobile component and one from a rigid component. The former displays Lorentzian decay and the latter displays Gaussian decay. The peak width of the spectrum is inversely proportional to the spin–spin relaxation time ( $T_2$ ) of the fluid phase. Both are highly responsive to changes in the molecular mobility, and this can be investigated as a function of temperature and interpreted in terms of chain scission and crosslinking. For example, in a study of the relationship between flammability and structure in a series of urethane-modified polyisocyanurates, we found that both differential scanning calorimetry (DSC) and high-temperature <sup>1</sup>H-NMR data clearly indicated that there were two major scission processes occurring within the polymers.<sup>28</sup>

The lower temperature process was due to the scission of the urethane links, whereas the higher temperature process, which became increasingly significant as the isocyanurate content of the polymer increased, was due to the scission of isocyanurate linkages. In addition, <sup>13</sup>C-NMR data on the residues clearly showed that the polyol was lost preferentially from those materials with the highest urethane/isocyanate ratio. The different fire performances of the four foams under study were thus ascribed to a conjunction of factors, all associated with the evolution of polyol or polyol fragments. First, the lower thermal stability of the urethane links led to facile depolymerization to yield free polyol from those foams where urethane linkages dominated over isocyanurate linkages. Second, the more rigid crosslinked network of the predominately isocyanurate linked foams restricted the diffusion of volatile species formed by and subsequent to the scission of any urethane bonds or the glycol backbone. In this article, we report the use of similar analytical methods, in particular, solid-state <sup>1</sup>H-NMR and solid-state <sup>13</sup>C-NMR to characterize the relationship between burning behavior and condensed-phase chemistry for two commercial PU samples.

## EXPERIMENTAL

### Materials

Two commercial flexible PU foams were supplied by Huntsman Polyurethanes (Everberg, Belgium), a on-combustion-modified high-resilience PU foam (CL592) and a combustion-modified high-resilience PU foam containing melamine and TCPP (CL594). The base foam formulation in each case was that of a standard high-resilience flexible foam comprising approximately 62 mass % of a poly(ethylene oxide)/poly(propylene oxide) copolymer and approximately 38 wt % of a polymeric MDI species of various functionalities with water and foaming additives. Although they were nominally PU foams, the materials were better described as polyureas, with urea rather than urethane links as the dominant species.<sup>30</sup>

### Limited oxygen index (LOI)

LOI tests were carried out at the Huntsman Polyurethanes Technology Centre. The standard procedure ASTM D 2863-91 was used. A mixture of oxygen and nitrogen of known composition was metered into the bottom of a tube passing through a bed of glass beads that smoothed the flow. The depth of the bed was between 80 and 100 mm, and the diameter of the beads varied from 3 to 5 mm. The foam was ignited at the upper end with a flame, which was then removed. The atmosphere that just permitted a steady burning down of the sample was determined.

### Motor vehicle safety standard test MV SS 302

MV SS 302 tests were carried out at Centexbel in Gent, Belgium.

This test was designed for the car industry and measured the rate of flame spread on a sample taken from the passenger compartment. The dimensions of the sample were  $356 \times 100 \times 13$  mm with reference marks at 38 and 292 mm. The sample was clamped between two U frames, placed in a horizontal position in a combustion chamber, and exposed to the flame of a Bunsen burner.

The flame was removed after 15 s, and the test ended when the second mark was reached or when the combustion stopped spontaneously. The combustion time was measured, and the flame spread was determined. The maximum allowed flame spread rate was 101.6 mm/min.

### American Standard California 117 test (CAL 117)

The CAL 117 tests were carried at Centexbel.

CAL 117 was a small-scale test used for the determination of resistance against flame, glow propagation, and tendency to char. The foam, with dimensions of  $305 \times 76 \times 13$  mm, was suspended in a vertical holder and exposed to a gas burner placed at the lower edge of the specimen. The flame was removed after 12 s. Afterward, the time needed to extinguish was measured. The pass criteria were

- The average char length of all specimens did not exceed 15 cm.
- The maximum char length of any individual specimen did not exceed 20 cm.
- The average afterflame, including the one of molten or dropped material, did not exceed 5 s.
- The maximum afterflame of any individual specimen, including the one of molten or dropped material, did not exceed 10 s.
- The average afterglow, including the one of molten or dropped material, did not exceed 15 s.

### British Standard BS 5852 test (BS 5852–Crib ignition source 5)

The BS 5852 Crib 5 tests were carried out at Centexbel.

The BS 5852 Crib 5 fire test was an assessment of the ignitability of upholstered seating by a flaming ignition source. Two pieces of foam of the dimensions  $450 \times 450 \times 75$  mm and  $450 \times 300 \times 75$  mm were assembled together on a frame and recovered on a fabric cover (100% Trevira CS) to form a seat. A wooden crib (constituted of 20 wooden pieces of dimension  $40 \times 6.5 \times 6.5$  mm) was placed in the cen-

tered position of the seat, also touching the back seat, and ignited with 1.4 mL of isopropyl alcohol. The duration of the test was 1 h. A sample would fail the test for the following reasons:

- It showed escalating flame combustion behavior.
- It burned until it was essentially consumed within the test duration.
- The flame front reached the extremities of the sample over the top of the vertical part of the sample or passed through the full thickness of the sample within the duration of the test.
- It showed continuing flaming for more than 10 min after ignition of the crib.

### DSC

DSC experiments were carried out with a DuPont 910 differential scanning calorimeter coupled with a DuPont 9900 computer/thermal analyzer. Indium was used as a calibration standard. Foams were placed and lightly compressed into an aluminum pan, which was then sealed with a pierced lid. The mass of the sample was between 5 and 7 mg. The reference pan corresponded to an empty pan plus a lid. Samples were heated from 50 to 550°C at 10°C/min under different atmospheres (i.e., nitrogen and a mixture of 3% oxygen in nitrogen) at a flow rate of 80 mL/min.

### Pyrolysis

The carbonaceous residues were prepared in a purpose-built pyrolysis apparatus comprised of a degradation vessel, a cold ring cooled with cold water, and two traps cooled with a bath containing a mixture of isopropyl alcohol and dry ice. About 200 mg of foam was placed inside a crucible, which was positioned in the center of the reactor. The furnace (Carbolite MTF 10/25/130 tube furnace with a 2416CC controller) was preheated at the desired working temperature under nitrogen or 3% oxygen in nitrogen at a flow rate of 250 mL/min before sample insertion. The sample was then inserted into the furnace for 20 min and then withdrawn from the reactor and cooled at ambient temperature. The volatile products present in the cold ring and in the two traps were collected with dichloromethane.

### Solid-state $^{13}\text{C}$ -NMR

A Bruker 200 DX spectrometer operating at 50 MHz was used for the solid-state  $^{13}\text{C}$ -NMR experiments. The two techniques of single pulse excitation (SPE) and cross-polarization/magic-angle spinning (CP-MAS) were used for each sample. Finely ground

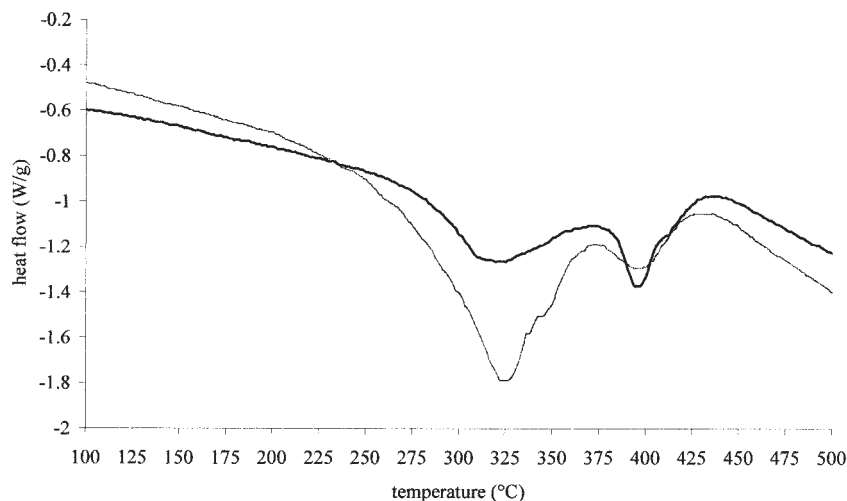


Figure 1 DSC curves obtained under nitrogen for the CL592 (darker line) and CL594 (lighter line) foams.

250 mg samples were inserted inside zirconia rotors with Kel-F caps. The CP-MAS technique was carried out with a magic-angle spinning of 5 kHz. All spectra were processed with a line-broadening factor of 50 Hz. The recycle delay between the successive contact times for each experiment was 2 s, and at least 1800 scans were accumulated. For each experiment, contact times of 1 and 5 ms were used; the maximum signal intensity was observed for a contact time of 1 ms. Tetakis(trimethylsilyl)silane was used as an internal standard (with a peak at 3.2 ppm). SPE experiments were carried out with a line-broadening factor of 50 Hz, a recycle delay of 60 s, and a contact time of 1  $\mu$ s. At least 1000 scans were obtained for each experiment. Dipolar dephasing experiments were also carried out to determine the percentage of protonated and non-protonated carbons present. Two dephasing times were used: 1 and 25  $\mu$ s. The first dephasing time generated the total carbon spectrum, and the second one generated the nonprotonated aromatic carbons.

#### High-temperature *in situ* solid-state $^1\text{H-NMR}$

A 100-MHz Doty (Columbia, SC) NMR probe was used along with the Bruker (Rheinstetten, Germany) 200 DX spectrometer. About 50 mg of finely ground

foam was packed into a container of boron nitride composition that was protected with an outer container composed of zirconia. The system was closed with a boron nitride screw. The whole assembly was placed horizontally into a stator composed of zirconia. The temperature of the sample was simultaneously monitored with two thermocouples, one touching the container of the sample and the other placed adjacent to the heater. The heat was transferred from the probe heater to the sample region with a flow of 12 L/min of dry nitrogen. Spectra were obtained at various temperatures between ambient temperature and 500°C, with the appropriate 90° pulse width and a solid echo pulse sequence (90°- $\tau$ -90°). The 90° pulse width varied between 2.2  $\mu$ s at ambient temperature and 2.9  $\mu$ s at 500°C. About 64 scans were obtained with a recycle delay between 0.9 and 14.6 s. The recycle delay was determined after each change of temperature by an inversion recovery experiment. The data from the spectrometer were then transferred to a computer (Power Mac 6000). The free-induction decay was obtained with a program called WinNMR 3.1 (Bruker). The resulting spectral data were saved in ASCII code and were finally opened in Microsoft Excel 4.0. The proton NMR spectrum was then represented by data points. The numerical data could be analyzed with an

TABLE I  
Peak Temperature Values from the DSC Curves Obtained Under Nitrogen and Under a Mixture of 3% Oxygen in Nitrogen for the CL592 and CL594 Foams

Sample	Atmosphere	Peak 1 (°C)	Peak 2 (°C)	Peak 3 (°C)	Peak 4 (°C)
CL592	N <sub>2</sub>	320 (endo)	397 (endo)	—	—
CL594	N <sub>2</sub>	325 (endo)	398 (endo)	—	—
CL592	3% O <sub>2</sub> /N <sub>2</sub>	286 (exo)	409 (exo)	—	—
CL594	3% O <sub>2</sub> /N <sub>2</sub>	266 (exo)	281 (exo)	321 (endo)	403 (exo)

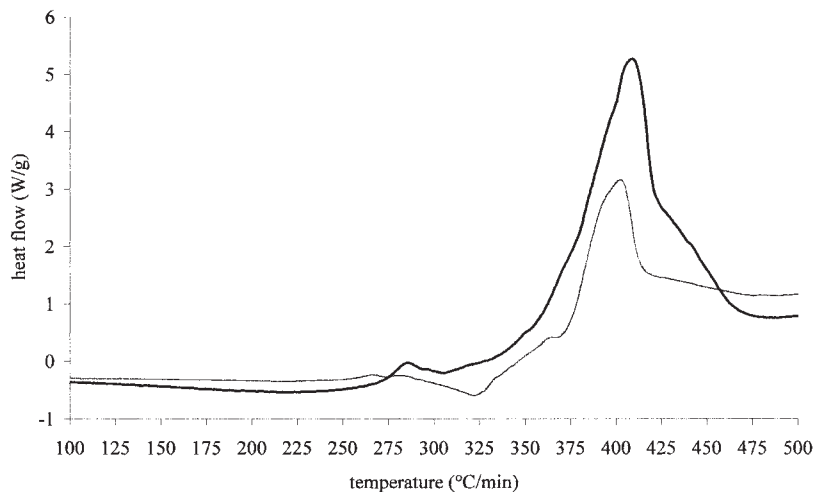


**Figure 2** DSC curves obtained under 3% oxygen in nitrogen for the CL592 (darker line) and CL594 (lighter line) foams.

in-house program called SIMFIT. This program allowed the fitting of the Lorentzian and Gaussian components to the original spectrum by numerical calculations.

#### Fourier transform infrared (FTIR) spectroscopy

FTIR analyses were performed using a Nicolet 410 spectrometer with Omnic Basic FTIR software

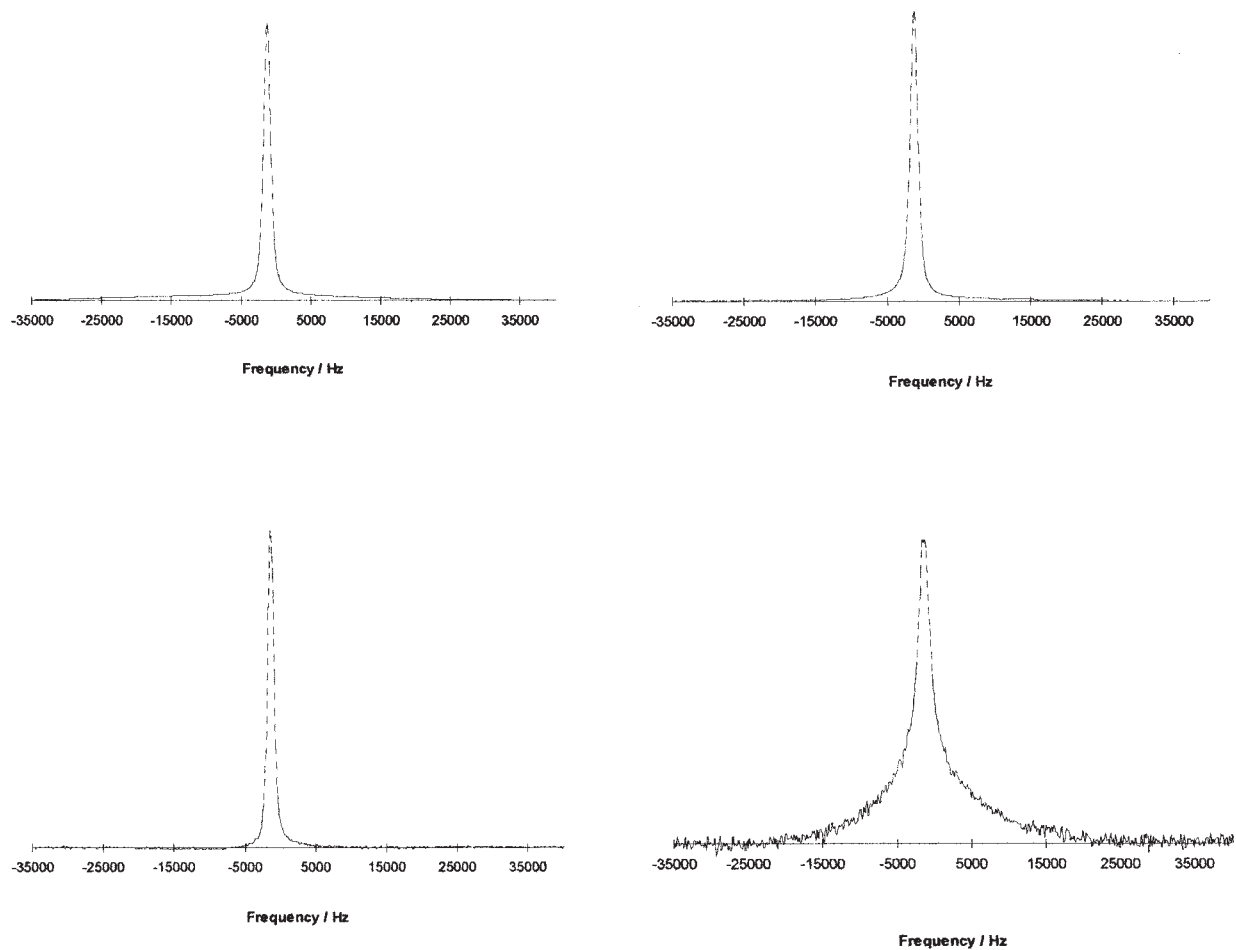


**Figure 3** Room-temperature, solid-state  $^1\text{H-NMR}$  spectra (top) of the CL592 (left) and CL594 (right) foams and the corresponding spectra obtained at 400°C (bottom) for the CL592 (left) and CL594 (right) foams.

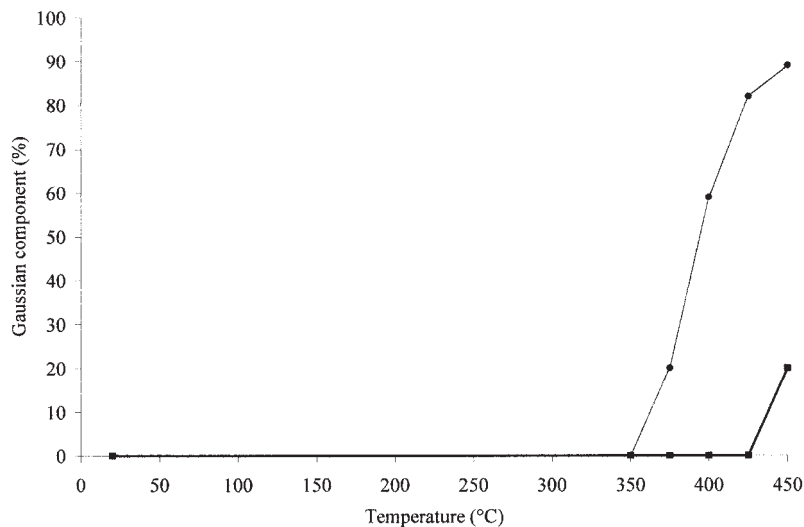


**Figure 4** Evolution of the Gaussian component (i.e., rigid protons) as a function of the temperature for the CL592 (darker line) and CL594 (lighter line) foams.

(Thermo Electron Corporation, Waltham, MA). Typically, 64 FTIR scans were accumulated with a resolution of  $4\text{ cm}^{-1}$ . Automatic smoothing and automatic baseline protocols were employed.

#### Elemental microanalyses

Elemental microanalyses were carried out by the microanalytical service within the University of Strathclyde.

## RESULTS AND DISCUSSION

### Combustion tests

The LOI values for these samples showed an effect of the melamine/TCPP formulation on the flammability of the foam. The CL592 foam had a lower LOI (21.3) than the CL594 foam (27.1), which implied that the melamine/TCPP formulation of CL594 reduced the flammability of the foam.

For the MVSS 302 test, three specimens from the CL592 foam and the CL594 foam were tested. Both foams passed the test; as in all cases, the foam stopped burning before it had burned for more than 60 s from ignition and had not burned more than 50 mm from the point of ignition. However, differences in flame propagation were observed between the two foams. The flame was applied under the foam, and for the CL592 foam, the flame propagated in both sides of the foam (i.e., the lower horizontal side and the upper horizontal side). In the CL594 foam, the propagation of the flame occurred only on the side where the Bunsen burner was applied (i.e., the lower horizontal side).

For the CAL 117 test, five specimens from each foam were tested. The average burn length was 82 mm for

CL592 and 68 mm for CL594. Both samples, therefore, passed the CAL 117 test, although CL594 clearly had an advantage over CL592. The shapes obtained after each sample was burned were different, which again indicated a different process of flame propagation. For the CL592 foam, the burning occurred vertically and also horizontally. The shape of the mark left after burning was similar to the shape of the flame. For the combustion-modified foam, CL594, the burning pattern was more symmetrical and parallel. This may have been related to the greater propensity of CL592 to melt drip.

The most challenging test was the Crib 5 test, and here, the samples were clearly differentiated, with only CL594 passing the test, self-extinguishing after 182 s. In contrast, CL592 underwent escalating combustion and had to be extinguished with water after 135 s.

During the tests, the CL592 foam melted and dripped on the burning wooden crib and fed the crib fire. For the CL594 foam, this was much less noticeable.

Overall, the combustion tests clearly showed the importance of assessing the test results in their proper context and emphasized that no single test fully represented the fire performance. Both foams passed the MVSS 302 and CAL 117 tests but only CL594 passed the stringent Crib 5 test. Compliance with this test is a required fire safety level for foams used in domestic furniture and mattresses in the UK.

### DSC

The DSC behavior of the two foams was studied under nitrogen and under a mixture of 3% oxygen in nitro-

TABLE II  
Residue Yields on Pyrolysis

Sample	Pyrolysis conditions	Total residue (%)	Soluble residue (%)	Insoluble residue (%)
CL592	300°C, 3% O <sub>2</sub> /N <sub>2</sub>	77.9	45.6	32.3
CL594	300°C, 3% O <sub>2</sub> /N <sub>2</sub>	72	40.5	31.5
CL592	350°C, 3% O <sub>2</sub> /N <sub>2</sub>	26.5	1	25.5
CL594	350°C, 3% O <sub>2</sub> /N <sub>2</sub>	39.1	6.4	32.7
CL592	350°C, N <sub>2</sub>	59.5	37.3	22.2
CL594	350°C, N <sub>2</sub>	55.3	25.6	29.7

The data are presented as percentages of the original sample mass.

gen. The DSC curves for the samples investigated under a nitrogen atmosphere are shown in Figure 1, and Table I summarizes the values of peak temperature from the DSC scans for each sample. The thermal degradation of both foams under nitrogen was endothermic and occurred in two steps. The first step corresponded to the scission of urea bonds at about 320°C, whereas the second step at about 397°C was associated with the degradation of the polyol sequences. CL594 showed a larger endothermic peak than CL592 in the urea bond decomposition region (i.e., ca. 320°C). Other results<sup>14</sup> indicate that when melamine was heated alone at 10°C/min, it started subliming at 315°C with a maximum rate of mass loss at 380°C. Our own DSC data showed melamine to sublime with the peak temperature at 318°C and an enthalpy change of approximately 900 J/g. It was possible, therefore, that in the foam, some melamine was subliming in the region of the urea bond decomposition and thus contributing to the endothermic peak and acting as a heat sink.

Even under a low concentration of oxygen (representative of the highly vitiated conditions in a fire), the overall thermal degradation of all of the samples was

TABLE III  
Microanalytical Data of the CL592 and CL594 Foams and Their Chars Obtained at 350°C under 3% Oxygen in Nitrogen

Sample	C (%)	H (%)	N (%)	O (%)	Cl (%)	P (%)
CL592	64.83	8.46	4.24	22.34	—	—
Char CL592	72.63	5.18	8.20	13.99	—	—
CL594	58.26	7.75	14.39	18.57	0.72	0.31
Char CL594	69.20	5.09	13.23	12.03	0	0.45

highly exothermic (Fig. 2). The peak temperature values for each DSC curve are summarized in Table I. In the presence of oxygen, the thermal degradation of CL592 was described in essentially two steps (the breakdown of the urea bonds and the thermooxidation of the polyol). Oxidation commenced immediately after the onset of the urea bond scission (at 286°C) when the decrease in molecular mass led to an increase in the chain mobility and a commensurate increase in oxygen diffusion through the polymer matrix. The major oxidation process dominating around 400°C was believed to be the thermooxidation of the polyol sequences.<sup>31,32</sup> The CL594 foam showed a similar degradation pathway to the nonmodified CL592 foam, but the first exotherm seemed to be greatly reduced, and an endothermic peak was observed just after (i.e., 321°C). This again suggested that melamine had a role as a heat sink, although the effect was small relative to the highly exothermic nature of the overall process.

#### Solid-state <sup>1</sup>H-NMR

The samples were examined with the temperature-resolved *in situ* solid-state <sup>1</sup>H-NMR technique from room temperature to 500°C to assess the hydrogen distribution and changes in the mobility of the polymer (selected spectra at room temperature and 400°C are shown in Fig. 3). All spectra were deconvoluted to determine the contribution to from the rigid Gaussian

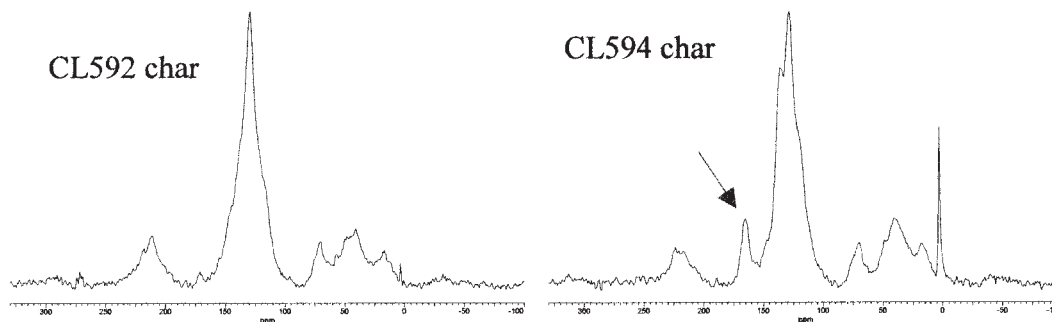


Figure 5 CP-MAS spectra (contact time = 1 ms) of the chars obtained at 350°C under 3% oxygen in nitrogen (the soluble products were extracted with dichloromethane).

**TABLE IV**  
**Percentage of Aromatic Carbons (mol % C) for the CL592 and CL594 Foams and Their Chars Obtained at 350°C under 3% Oxygen in Air**

	Sample	
	CL592	CL594
Undegraded foam (calculated)	40	50
Char (determined from CP-MAS)	87	84

The carbonyl group was included with  $sp^2$  carbons.

component and the mobile Lorentzian component, and Figure 4 shows the evolution of the Gaussian component (i.e., rigid protons) as a function of temperature for both foams. The samples behaved similarly from room temperature to 350°C, with the polymer molecules being fully mobile. However, by 375°C, the CL594 foam became markedly less fluid, and by 450°C, the CL594 foam was nearly fully rigid. The CL592 foam developed a rigid component only above 400°C. This was similar to the observation in our earlier study<sup>17</sup> and was consistent with the observation from the Crib 5 test that the CL594 foam was much less prone to melt flow and drip than the CL592 foam.

### Pyrolysis

Pyrolyses at 350°C (i.e., just at the point of differentiation between CL592 and CL594 in the temperature-resolved *in situ* solid-state  $^1\text{H-NMR}$  experiments) under nitrogen and under 3% oxygen in nitrogen produced residues that consisted of dichloromethane-soluble (tar) and dichloromethane-insoluble (char) components. These are quantified in Table II. In general, higher char yields are identified with lower flammability by virtue of the lower volatile feed to the flame zone. A comparison of the CL592 and CL594 foams showed that the combustion-modified foam had the

higher char fraction. A comparison of the data from the pyrolyses under nitrogen and under 3% oxygen in nitrogen was revealing and showed that for both the CL592 foam and the CL594 foam, gross residue yields were down, primarily at the expense of the tar component; this reflected the greater instability of the polyol component under oxidative conditions.<sup>31,32</sup>

The chars (i.e., the nonsoluble component of the residue) obtained at 350°C under 3% oxygen in nitrogen were characterized by solid-state CP-MAS  $^{13}\text{C-NMR}$  (Fig. 5). Overall, all the chars mainly consisted of aromatic carbons (peak at 136 ppm). Only a small amount of polyol still remained in the char (peaks at 16 and 69 ppm). The CL594 char possessed an extra peak at 167 ppm, which could have been due to the presence of melamine or derived moieties. This was in accordance with the microanalytical data, which showed a high nitrogen content (Table III). The percentages of aromatic carbons in the chars were determined by integration of the CP-MAS spectra and compared with the undegraded foams (see Table IV). The ratio of aromatic to aliphatic carbons varied between 40:60 and 50:50 for the original foams, and a considerable increase in aromatic carbon content was observed, which confirmed the volatilization of the polyol. In addition, dipolar dephasing experiments were undertaken for the chars from the CL592 and CL594 foams. This technique allowed us to determine the percentage of nonprotonated aromatic carbons. The fraction of total aromatic carbons that were not protonated was slightly higher in the char from the CL594 foam (83%) than in the char from the CL592 foam (74%). This may have been due to residual melamine, although it could have indicated some condensation of the aromatic species

The tars and condensed volatile products from the 3% oxygen in nitrogen pyrolyses were analyzed by FTIR and solution NMR and were similar in both

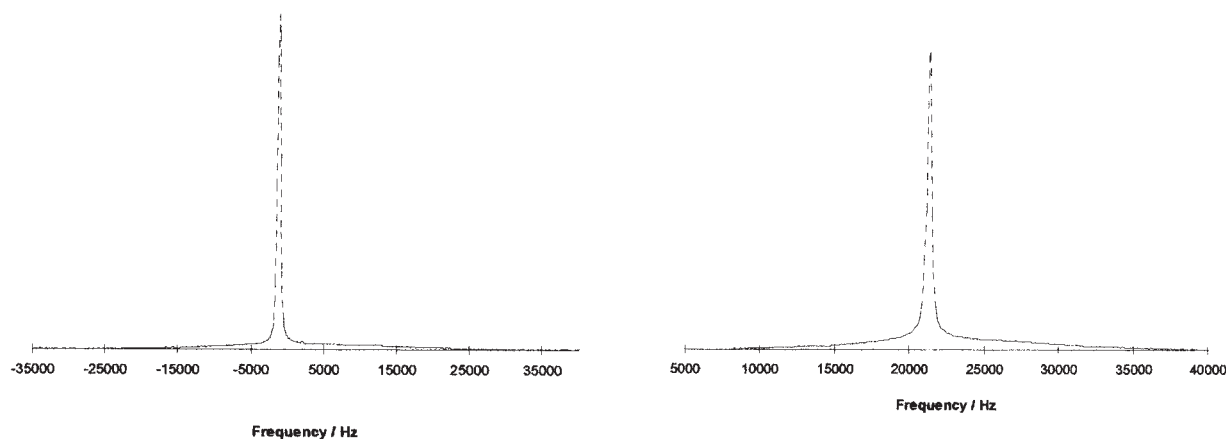


**Figure 6** Broad-line  $^1\text{H-NMR}$  spectra of the CL592 (left) and CL594 (right) chars collected after the BS5852 Crib 5 fire test.



**TABLE V**  
**Percentage of Rigid and Mobile Protons (Gaussian and Lorentzian Components, Respectively) and Their Respective  $T_2$  Values**

Sample	Gaussian (%)	Lorentzian (%)	$T_2$ ( $\mu$ s)	
			Gaussian	Lorentzian
CL592	0	100	— <sup>a</sup>	333
CL594	0	100	— <sup>a</sup>	270
Combustion Char CL592	26	74	19	640
Combustion Char CL594	50	50	37	932

<sup>a</sup> Foam was completely fluid.

cases; typically, they were mostly polyol with some urethane and urea structures, some aromatic structures (possibly including primary amines), and in the case of CL594, some sublimed melamine.

#### Characterization of residues from the Crib 5 test

The residues (i.e., the top 2 mm of the degraded foams) were carefully separated from the bulk material and extracted with dichloromethane. The extractable products (tars) were analyzed by FTIR and

solution-state  $^1\text{H-NMR}$  and  $^{13}\text{C-NMR}$ . The insoluble products (chars) were studied by solid-state  $^1\text{H}$  and  $^{13}\text{C-NMR}$  and elemental analysis. The tar products from both foams were very similar and were predominantly polyol sequences, although there were some urethane/urea structures and rather more aromatic fragments in the tar from the CL594 foam.

Solid-state  $^1\text{H-NMR}$  (at room temperature) was carried out on both combustion chars (see Fig. 6) and compared to the spectra of the nondegraded foams (see Fig. 3). As noted earlier, at room temperature, the molecules in both undegraded CL592 and CL594 were highly mobile, and the NMR lineshape was entirely Lorentzian (Table V). In contrast, the combustion chars showed a significant Gaussian (rigid) component, with CL594 having a greater rigid content albeit with more mobile molecules within both the mobile and rigid environments (i.e., longer  $T_2$ ). These results were consistent with the condensed-phase crosslinking action of melamine.<sup>17</sup>

The continued presence of melamine in the CL594 residue was demonstrated by the CP-MAS  $^{13}\text{C-NMR}$  characterization of the chars (Fig. 7). The CP-MAS spectra of the combustion chars from CL592 and CL594 showed both chars to be highly aromatic with only a small amount of polyol still present. However, the peak at 167 ppm for the char from the CL594 sample was indicative of melamine. Microanalysis

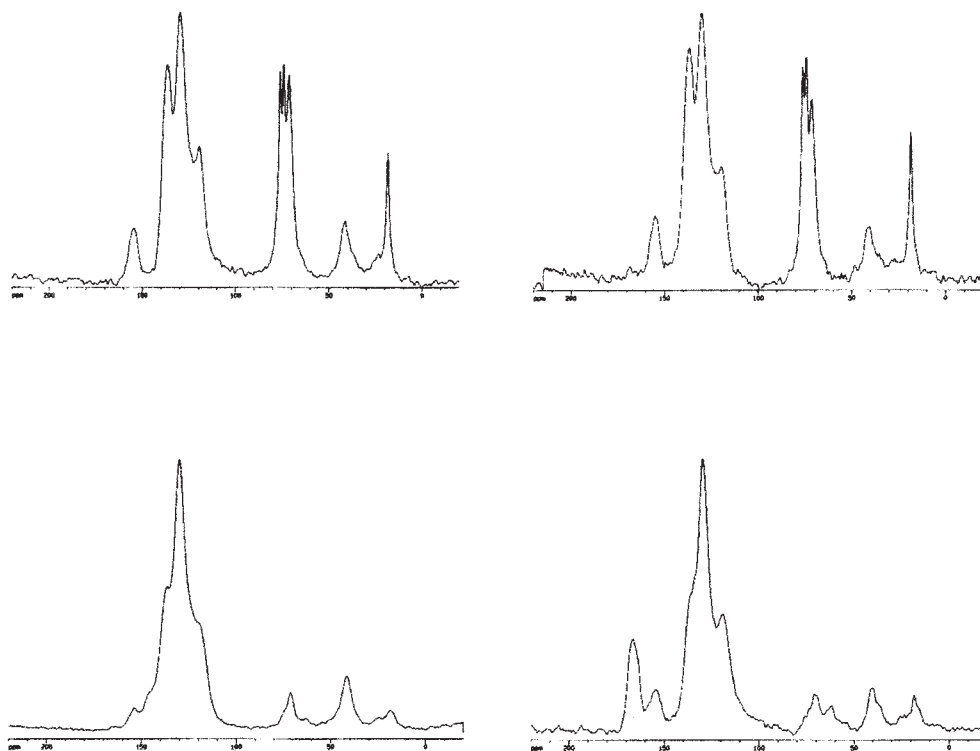


**Figure 7** CP-MAS spectra at room temperature for the CL592 (top left) and CL594 (top right) foams and the combustion chars from the Crib 5 fire test for the CL592 (bottom left) and CL594 (bottom right) foams.

**TABLE VI**  
**Microanalytical Data for the CL592 and CL594 Foams**  
**and Their Chars Collected from the Crib 5 Fire Test**

Sample	C	N	H	O	P	Cl
CL592 foam	64.93	4.27	8.46	22.34	—	—
CL592 char	73.18	10.17	5.95	10.7	—	—
CL594 foam	58.26	14.39	7.75	18.57	0.31	0.72
CL594 char	47.14	39.71	5.26	7.59	0.30	Trace/nil

confirmed a high nitrogen content in the CL594 char (Table VI). Some phosphorous, but no chlorine, from the TCPP was present; this was consistent with the known degradation pathway of TCPP, in which chlorine is lost as HCl or vinyl chloride.<sup>18</sup>

### CONCLUSIONS

The combustion tests showed that the foams met several regulatory requirements in terms of their fire performance, whether or not they were combustion-modified. Both foams passed the MV SS 302 and CAL 117 small-flame tests. The nonmodified foam failed the Crib 5 test, but this test had a much larger ignition source. The particular problem with the nonmodified CL592 foam was melt drip into the flame zone. This led to a steady maintenance of the fuel feed and a rapid escalation of the fire. In contrast, the combustion-modified CL594 foam showed little melt drip and self-extinguished. The DSC data for the two foams under both N<sub>2</sub> and 3% O<sub>2</sub> in N<sub>2</sub> showed that melamine acted, at least in part, as an endothermic heat sink. This alone did not account for the much reduced melt flow and drip of the combustion-modified foam, but the solid-state <sup>1</sup>H-NMR data clearly showed that the molecular mobility of the combustion char from the combustion-modified foam was much lower relative to the unmodified foam char, with twice as great an immobile Gaussian component. The *in situ* solid-state <sup>1</sup>H-NMR experiments, in which the foams were heated in the spectrometer, also clearly showed that CL594 underwent more pronounced crosslinking, with the onset of immobile char formation occurring some 75°C lower than for CL592. Clearly, therefore, the flame-retardant formulation in CL594 had an effective condensed-phase action. Solid-state <sup>13</sup>C analysis showed the continued presence of melamine in the combustion char from CL592, and microanalysis showed residual phosphorous. It seems, therefore, that the crosslinking chemistry resulted from the interaction of melamine with the matrix, as we proposed earlier,<sup>17</sup> coupled with a contribution from a phosphoric acid derived crosslinking mechanism.<sup>18</sup>

### References

- Morikawa, T.; Yanai, E.; Okada, T.; Watanabe, T.; Saito, Y. *Fire Safety J* 1993, 20, 257.
- Grassie, N.; Zulfiqar, M. *J Polym Sci Polym Chem Ed* 1978, 16, 1563.
- Grassie, N.; Perdomo Mendoza, G. A. *Polym Degrad Stab* 1985, 10, 267.
- Ravey, M.; Pearce, E. M. *J Appl Polym Sci* 1997 63, 47.
- Herzog, K. *Makromol Chem Macromol Symp* 1991, 52, 307.
- Jeffs, G. M.; Sand, H. *Cell Polym* 1984, 3, 401.
- Gaboriaud, F.; Vantelon, J. P.; Breillat, C. *J Polym Sci Polym Chem Ed* 1982, 20, 2063.
- Horrocks, A. R.; Price, D.; Edwards, N. L. C. *J Fire Sci* 1992, 10, 28.
- Horrocks, A. R.; Price, D.; Edwards, N. L. C. *Makromol Chem Macromol Symp* 1993, 74, 315.
- Dufton, P. W. *Fire-Additives and Materials*; Rapra Technology: Shrewsbury, England, 1995.
- Barker, M.; Hannaby, M. P.; Lockwood, F. J. In *Proceedings of the Polyurethanes World Congress 1991*, Technomic: Lancaster, PA, Sept 1991; p 628.
- Horacek, H.; Grabner, W. *Makromol Chem Macromol Symp* 1993, 74, 271.
- Knaub, P. H.; Mispereuve, H. In *Proceedings of the 32nd Annual Polyurethane Technical/Marketing Conference*, Technomic: Lancaster, PA, Oct 1989; p 501.
- Costa, L.; Camino, G. *J Therm Anal* 1988, 34, 423.
- Costa, L.; Camino, G.; Luda di Cortemiglia, M. P. In *Fire and Polymers*; Nelson, G. L., Eds.; ACS Symposium Series 425; American Chemical Society: Washington, DC, 1990; p 211.
- Feng, D.; Zhou, Z.; Bo, M. *Polym Degrad Stab* 1995, 50, 65.
- Dick, C. M.; Denecker, C.; Liggat, J. J.; Mohammed, M. H.; Snape, C. E.; Seeley, G.; Lindsay, C.; Eling, B.; Chaffanjon, P. *Polym Int* 2000, 49, 1177.
- Matuschek, G. *Thermochim Acta* 1995, 263, 59.
- Miyazawa, K.; Yokono, T.; Sanada, Y. *Carbon* 1979, 17, 223.
- Maciel, G. E.; Bartuska, V. J.; Miknis, F. P. *Fuel* 1979, 58, 391.
- Maciel, G. E.; Sullivan, M. J.; Petrakis, L.; Grandy, D. W. *Fuel* 1982, 61, 411.
- Earl, W. L.; Van der Hart, D. L. *J Magn Res* 1982, 48, 35.
- Maroto-Valer, M. M.; Andresen, J. M.; Rocha, J. D.; Snape, C. E. *Fuel* 1996, 75, 1721.
- Maroto-Valer, M. M.; Andresen, J. M.; Snape, C. E. *Energy Fuels* 1997, 11, 236.
- Bourbigot, S.; Le Bras, M.; Delobel, R.; Decressain, R.; Amoreux, J. P. *J Chem Soc Faraday Trans* 1996, 92, 149.
- Bourbigot, S.; Le Bras, M.; Delobel, R.; Tremillon, J. M. *J Chem Soc Faraday Trans* 1996, 92, 3435.
- Gilman, J. W.; Kashiwagi, T.; Lomakin, S.; Van der Hart, D. L.; Nagy, V. *Fire Mater* 1998, 22, 61.
- Dick, C. M.; Dominguez-Rosado, E.; Eling, B.; Liggat, J. J.; Lindsay, C. I.; Martin, S. C.; Mohammed, M. H.; Seeley, G.; Snape, C. E. *Polymer* 2001, 42, 913.
- Jiang, D. D.; Levchik, G. F.; Levchik, S. V.; Dick, C.; Liggat, J. J.; Snape, C. E.; Wilkie, C. A. *Polym Degrad Stab* 2000, 68, 75.
- The Polyurethanes Handbook*, 2nd ed.; Randall, D.; Lee, S., Eds.; Wiley: New York, 2003.
- Costa, L.; Camino, G.; Luda, M. P.; Cameron, G. G.; Qureshi, M. Y. *Polym Degrad Stab* 1996, 55, 301.
- Costa, L.; Gad, A. M.; Camino, G.; Cameron, G. G.; Qureshi, M. Y. *Macromolecules* 1992, 25, 5512.